

Local structure around Mn atoms in Si crystals implanted with Mn⁺ studied using x-ray absorption spectroscopy techniques

A. Wolska, K. Lawniczak-Jablonska, M. Klepka, and M. S. Walczak
Institute of Physics, PAS, Aleja Lotnikow 32/46, 02-668 Warsaw, Poland

A. Misiuk
Institute of Electron Technology, Aleja Lotnikow 46, 02-668 Warsaw, Poland

(Received 13 October 2006; revised manuscript received 15 December 2006; published 1 March 2007)

The local order around Mn atoms in the Mn-implanted Si samples, with ferromagnetic properties, has been investigated by use of x-ray-absorption spectroscopy techniques. Analysis of both extended x-ray-absorption fine structure and x-ray absorption near-edge structure spectra clearly indicates that Mn ions are located neither in the substitutional nor in the interstitial position in the Si lattice, but depending on how the samples were prepared, they have five to eight near neighbors.

DOI: [10.1103/PhysRevB.75.113201](https://doi.org/10.1103/PhysRevB.75.113201)

PACS number(s): 61.72.Tt, 61.10.Ht, 78.70.Dm

Mn-doped III-V and II-VI compounds forming diluted magnetic semiconductors (DMSs) have been extensively investigated in pursuit of ferromagnetic materials, which can be used in spintronic devices.¹ On the other hand, Si-based DMSs have not been fully examined despite the advantage that any potential spintronic device based on silicon would be easy to integrate with the existing technologies. Among Si-based DMSs, those implanted with Mn appear to be particularly promising materials. Bolduc *et al.*² have discovered that the Mn-implanted Si samples are ferromagnetic and have a Curie temperature (T_C) higher than 400 K.

There are several reports devoted to Mn⁺ implanted within a silicon matrix. They are mainly focused on the concentration of Mn atoms. Egamberdiev and Adylov³ showed that concentrations of manganese and oxygen atoms are anticorrelated, which suggests that Mn ions do not bond with oxygen and do not form oxides. Francois-Saint-Cyr *et al.*⁴ measured the dependence of Mn diffusion on annealing temperature, showing that Mn atoms tend to diffuse to the surface if the temperature is higher than 770 °C. However, the local surroundings around the Mn atoms in such systems is still unresolved.

This Brief Report shows the results of the analysis of x-ray-absorption spectra of Mn⁺ implanted into Si samples. This technique is sensitive to one (selected) atomic species only and provides important information about the atomic and electronic structures.

To obtain information on the influence of sample-processing conditions on the location of implanted Mn in Si crystals, three kinds of (001) oriented Si:Mn samples were prepared by Mn⁺ implantation into Si. The first one, marked by sim0, was prepared by implantation into Fz-Si (grown by the floating zone method) and the two others, marked by sim1 and sim3, were prepared by Mn⁺ implantation into Cz-Si (grown by the Czochralski method). The Mn⁺ ions with the energy of 160 keV were implanted into Si to a dose of $1 \times 10^{16} \text{ cm}^{-2}$ or, in the case of sim3, $1.2 \times 10^{16} \text{ cm}^{-2}$. The temperature of the Si substrate at implantation was kept at 340 K for sim1 and sim3, while it was set at 610 K for sim0. The projected Mn⁺ ion range in the implanted samples was about 100 nm. Interstitial oxygen concentrations in Fz-Si and

in Cz-Si samples were $\leq 1 \times 10^{17}$ and $9 \times 10^{17} \text{ cm}^{-3}$, respectively. Detailed structural characteristics of the samples as well as their magnetic data were reported elsewhere.^{5,6}

The x-ray-absorption near-edge structure (XANES) and extended x-ray-absorption fine structure (EXAFS) spectra were measured for all studied samples at the A1 station, Hasylab, Hamburg. The two-crystal Si (111) monochromator at the A1 station ensures a resolution of $\Delta E/E = 10^{-4}$. Measurements were carried out at the Mn *K* edge using the x-ray fluorescence detection method and a seven-element silicon detector. The samples were cooled to liquid-nitrogen temperature to minimize thermal disorder. Additional reference spectra of metallic Mn foil and Mn oxides were measured in the transmission mode.

Very little difference was found between the XANES spectra for all investigated samples; therefore, only one will be shown. The first step of XANES analysis was a comparison with the experimental spectra of manganese oxides and pure Mn metallic foil (Fig. 1). The difference between the spectra is substantial, which shows that Mn atoms form neither metallic nor oxide inclusions in the Mn-implanted Si samples. Moreover, the assumption that only a part of the Mn atoms oxidize or that the Mn atoms form different oxides

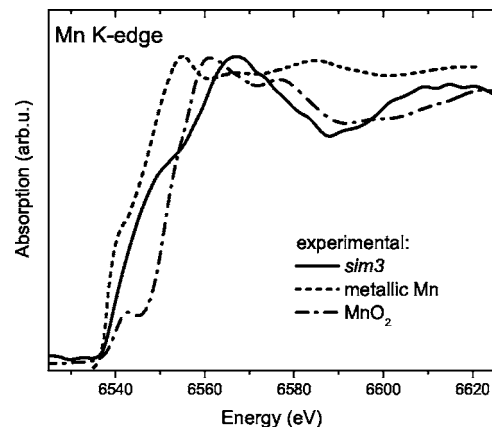


FIG. 1. XANES spectra for measured sample, metallic Mn, and MnO₂. The pronounced differences in the shape of the spectra allowed us to exclude the formation of oxides by implanted ions.

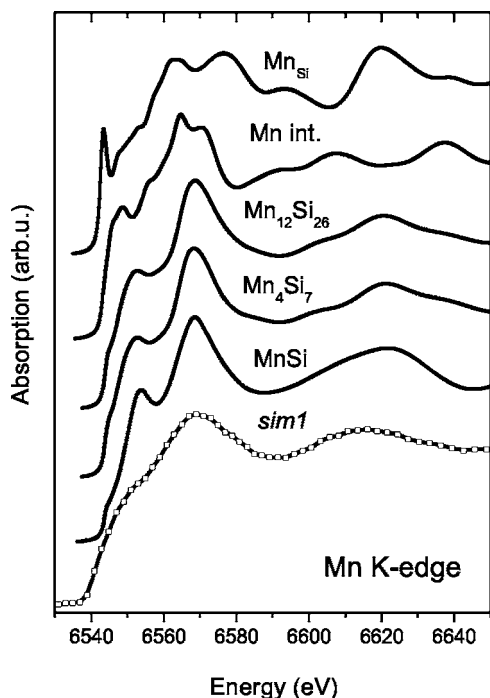


FIG. 2. Experimental spectrum for sample sim1 and XANES spectra calculated for different models of Mn location in the Si lattice: Mn_{Si} , substitutional; $Mn_{int.}$, interstitial; $Mn_{12}Si_{26}$, Mn_4Si_7 , and $MnSi$, the order as in crystalline Mn-Si compounds.

can also be ruled out since the first maxima in the reference spectra are shifted toward lower energy with respect to the experimental spectrum. This remains in agreement with the observation made from the Rutherford backscattering measurement showing that the maximum of manganese concentration is correlated with a minimum of oxygen concentration in similar samples.³

The FEFF 8.2 code⁷ enabling theoretical calculation of the x-ray absorption for different models was used in the estimation of the possible surroundings of the implanted Mn atoms. The Hedin-Lundqvist exchange correlation potential as well as the self-consistent-field, the XANES, and the full multiple scattering cards were applied in all cases. The cluster radii of 10 Å were used.

For the first set of XANES calculations, a perfect silicon matrix was used as a base. For the first model, the central Si atom was replaced by one Mn atom (substitutional model, Mn_{Si}). For the second model, the Mn atom was located in the interstitial position. As can be seen in Fig. 2, the calculated spectra of Mn_{Si} and Mn interstitial differ significantly from the experimental spectrum. Therefore, in the next set of calculations, the possibility for the formation of Mn_xSi_y inclusions was examined. In particular, crystallographic data for $MnSi$,⁸ Mn_4Si_7 ,⁹ and $Mn_{12}Si_{26}$ (Ref. 10) were used. In the case of compounds where Mn atoms are located in several nonequivalent sites, the calculations were performed for all of them and averaged with appropriate weights depending on the site symmetry. The obtained results are shown in Fig. 2. None of the considered compounds resembles the observed shape of the spectrum. The measured spectrum is broader and without fine structure, which should be observed in the

Mn-Si compounds. Due to the fact that in EXAFS analysis only the scattering amplitudes and phases and some starting geometry of atom positions are important, we have used the MnSi compound as a starting model for further analysis.

The ARTEMIS and ATHENA programs,¹¹ using the IFEFFIT data analysis package, were applied in the analysis of the EXAFS data. As can be seen in Figs. 3(b)–3(d), only the first shell is clearly visible for all of the experimental samples, suggesting high structural disorder or even a lack of long-range structural order around Mn atoms. A difference in the shape of the first peak suggests that the average Mn surroundings varies between the samples.

Analysis of each spectrum was carried out in the same manner. Only the first shell was considered. The coordination number (N) and passive electron reduction factor (S_0^2) cannot be fitted together. In order to break the correlation between them, one of these parameters had to be fixed. Since the XANES analysis showed that the number of nearest neighbors is not determined, it seemed justified to fix S_0^2 at some reasonable value such as 0.9, introducing an additional error in the value of N of about 10%.

The fitting procedure was started by using only single scattering paths on Si, Mn, or O atoms. Other paths were then added. In all the cases, the introduction of the oxygen paths led to unphysical parameters or resulted in serious deterioration of the fit. Considering only Mn as the nearest neighbor also led to unphysical results. Finally, the silicon paths were used. The results of the fitting procedure are collected in Table I and the final fit in the R space is shown in Figs. 3(b)–3(d). The third cumulant (parameter of asymmetry in the distribution of neighboring atoms) was introduced for some paths to improve the quality of the fit. Two scattering paths on silicon atoms and one on manganese were necessary to obtain a reasonable fit to experimental data for sim0. In the case of sim1 and sim3, one silicon path was sufficient.

It follows from the EXAFS analysis that in sim0, the sample prepared by the floating zone method followed by Mn ion implantation on a heated substrate, the manganese atoms formed clusters with 6–8 atoms located in the first coordination sphere in three subshells. In the case of crystalline $MnSi$, the first subshell (see Table I) has one atom at a distance of 2.31 Å, the second subshell has three at 2.4 Å, the third subshell has three atoms at 2.54 Å, and finally the fourth subshell contains six Mn atoms at a distance of 2.80 Å. For sim0, we found an average of 4.7 atoms at a larger distance of 2.45 Å in the first subshell, and for the second subshell we found 1.9 atoms at a distance of 2.59 Å. The largest difference was found in the third subshell with 1.5 Mn atoms at the distance of 2.71 Å. These results suggest that Mn in this sample exhibits a tendency to form a structure to some extent similar in coordination to that in manganese silicides such as $MnSi$, but due to the low concentration of Mn, the full structure cannot be completed. It seems highly probable that the Mn atoms introduced into the Si structure with high kinetic energy were stopped in a highly defected Si matrix, attracting five to seven Si atoms and started to form a manganese silicide compound.

For sim1 and sim3 samples, EXAFS analysis did not confirm the location of Mn in the neighborhood of the central absorbing Mn atom; only about five to eight Si atoms at

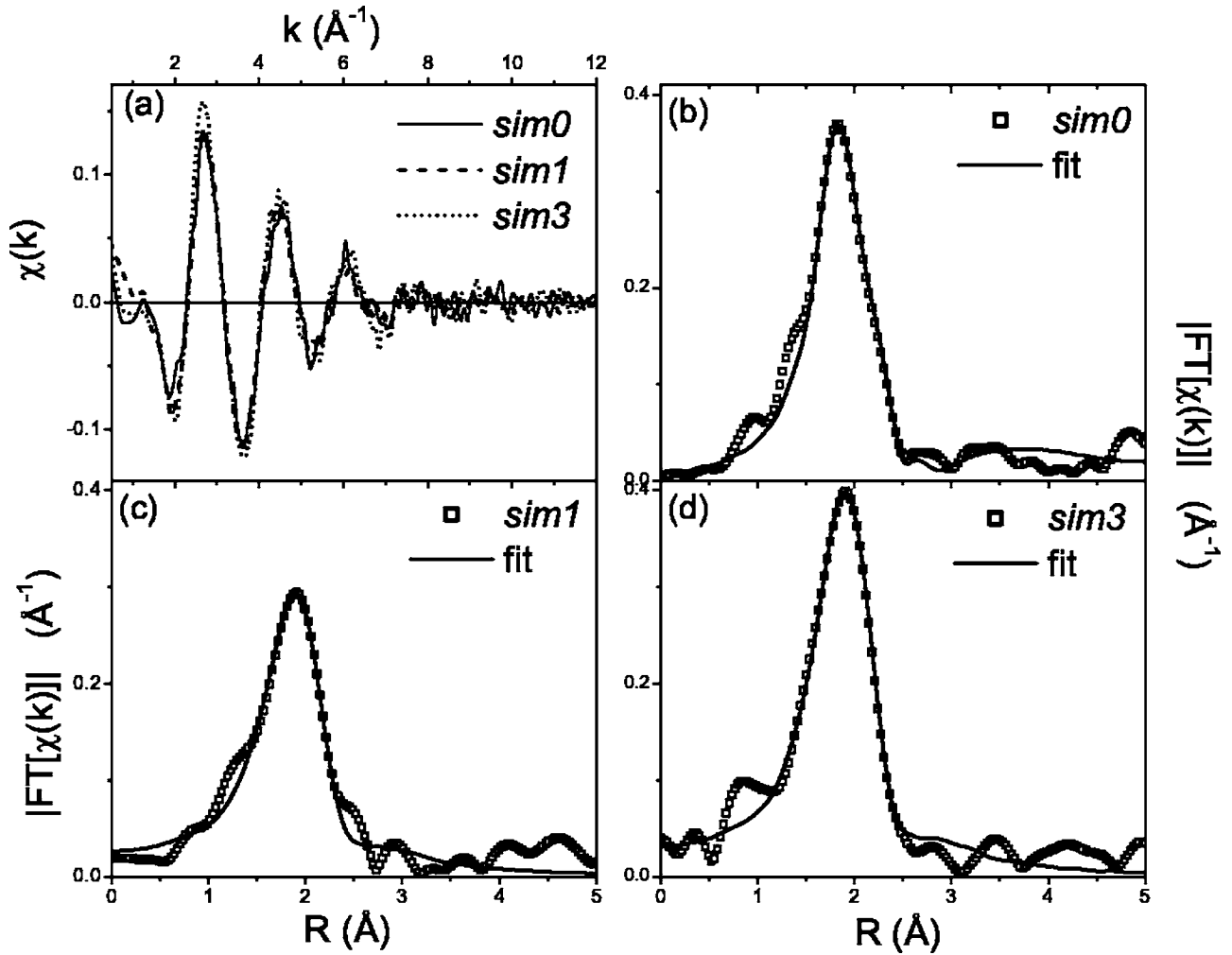


FIG. 3. (a) The raw $\chi(k)$ data of the investigated samples. [(b)–(d)] The Fourier transform of the data with the best fit.

distances of 2.42–2.43 Å were found. Therefore, we conclude that the changes in the dose of implanted Mn ions do not influence the Mn location, but rather it is the heating of the substrate during the implantation, which results in the forming of a more ordered structure around the implanted Mn ions.

Comparison of the atomic order around implanted Mn in the investigated samples with their magnetic properties, reported for the same samples in Refs. 5 and 6, indicates that the presence of a second Mn atom in the vicinity of the central Mn, as observed in sim0, enhances the ferromagnetic properties. The coercive field for sim0 was equal to 100 Oe

TABLE I. Results of fitting procedure to the experimental EXAFS spectra for the investigated samples and crystallographic data for stoichiometric MnSi (Ref. 8).

Sample	Type of atom	Coordination	r bond length (Å)	σ^2	Third cumulant	Fit factor R
sim0	Si	4.7+/-0.6	2.45+/-0.01	0.006+/-0.002	0.0018+/-0.0002	0.0067
	Si	1.9+/-0.8	2.59+/-0.01	0.006+/-0.002		
	Mn	1.5+/-0.3	2.71+/-0.03	0.009+/-0.002		
sim1	Si	6.2+/-0.7	2.42+/-0.04	0.011+/-0.002	0.0005+/-0.0008	0.0080
sim3	Si	7.4+/-0.5	2.43+/-0.02	0.009+/-0.001	0.0005+/-0.0003	0.0010
MnSi	Si	1	2.31			
	Si	3	2.40			
	Si	3	2.54			
	Mn	6	2.80			

and the weak temperature dependence of this field indicated that T_C exceeded 300 K. The two other samples we investigated exhibit a very weak ferromagnetic order at 5 K. It is well established that the spin dependent hybridization between anion (group IV) p and Mn d states leads to superexchange and a short-range antiferromagnetic coupling among the Mn moments.¹² Nevertheless, it has been found, by the model calculation,¹³ that the pairs of Mn spins coupled to the matrix valence band states have a lower energy in the ferromagnetic configuration than they would have in the antiferromagnetic one. Contrary to the results presented by Bolduc *et al.*,² we did not observe an influence of the conductivity type and concentration of carriers in the initial nonimplanted silicon on the magnetic ordering; therefore, this suggests that the magnetism in Mn-implanted Si may be of other origin than hole mediated. The model considered by Wolff *et al.*,¹⁴ which assumes carriers localized on impurities forming bound magnetic polarons with ferromagnetic coupling, seems to provide a better explanation. Obviously, this requires further investigation; of particular interest would be

studies of the structural order in samples with well-known magnetic and electrical properties.

In summary, the analysis of XANES and EXAFS spectra proved that Mn ions implanted into bulk silicon do not form either metallic or oxide inclusions. Moreover, the models assuming the location of Mn in the substitutional or interstitial position in the Si lattice, as was suggested in Ref. 15, result in theoretical spectra different from the experimental ones. Both XANES and EXAFS spectra are in reasonable agreement with the model, which assumes the formation of clusters with short-range order close to strained and defected Mn-Si compounds with five to eight near-neighbor atoms. Clusters formed in the sample with Mn implantation performed on a heated substrate, sim0, show the local order closer to that in the Mn-Si phases. This sample also exhibits better magnetic properties than the other samples investigated.

This work was partially supported by the Contract No. RII3-CT-2004-506008 (IASFS) of the European Commission.

-
- ¹S. A. Wolf, D. D. Awschalom, R. A. Buhrman, J. M. Daughton, S. von Molnar, M. L. Roukes, A. Y. Chtchelkanova, and D. M. Treger, *Science* **294**, 1488 (2001).
- ²M. Bolduc, C. Awo-Affouda, A. Stollenwerk, M. B. Huang, F. G. Ramos, G. Agnello, and V. P. LaBella, *Phys. Rev. B* **71**, 033302 (2005).
- ³B. E. Egamberdiev and M. Y. Adylov, *Tech. Phys. Lett.* **27**, 168 (2001).
- ⁴H. Francois-Saint-Cyr, E. Anoshkina, F. Stevie, L. Chow, K. Richardson, and D. Zhou, *J. Vac. Sci. Technol. B* **19**, 1769 (2001).
- ⁵A. Misiuk, B. Surma, J. Bak-Misiuk, A. Barcz, W. Jung, W. Osinniy, and A. Shalimov, *Mater. Sci. Semicond. Process.* **9**, 270 (2006).
- ⁶A. Misiuk, J. Bak-Misiuk, B. Surma, W. Osinniy, M. Szot, and T. Story, *J. Alloys Compd.* **423**, 201 (2006).
- ⁷A. L. Ankudinov, B. Ravel, J. J. Rehr, and S. D. Conradson, *Phys. Rev. B* **58**, 7565 (1998).
- ⁸T. M. Hayes, J. W. Allen, J. B. Boyce, and J. J. Hauser, *Phys. Rev. B* **23**, 4691 (1981).
- ⁹U. Gottlieb, A. Sulpice, B. Lambert-Andron, and O. Laborde, *J. Alloys Compd.* **361**, 13 (2003).
- ¹⁰H. W. Knott, M. H. Mueller, and L. Heaton, *Acta Crystallogr.* **23**, 549 (1967).
- ¹¹B. Ravel and M. Newville, *J. Synchrotron Radiat.* **12**, 537 (2005).
- ¹²T. Dietl, *Semicond. Sci. Technol.* **17**, 377 (2002).
- ¹³J. Inoue, S. Nonoyama, and H. Itoh, *Phys. Rev. Lett.* **85**, 4610 (2000).
- ¹⁴P. A. Wolff, R. N. Bhatt, and A. C. Durst, *J. Appl. Phys.* **79**, 5196 (1996).
- ¹⁵H. Nakayama, H. Ohta, and E. Kulatov, *Physica B* **302**, 419 (2001).